# Identification and Modeling of Polymeric Actuators: a comparison

Graziani S.[1], Umana E. [1], Xibilia M.G. [2], *Member, IEEE*

[1]*DIEEI, University of Catania, viale Andrea Doria 6, 95125 Catania*
[2]*DiSIA, University of Messina, Nuova Panoramica dello Stretto, 98166 Messina*
*mxibilia@unime.it*

***Abstract*—In this paper different strategies to model Ionic Polymer-Polymer Composite (IP$^2$C), used as actuator, are compared. Starting from some previous results regarding the ionic polymer metal composites (IPMCs) modeling, a linear gray-box model has been determined for an IP$^2$C actuator. Moreover linear and nonlinear black-box models have been identified from experimental data. A comparison among developed models has been performed in order to determine the model that better describes the actuator behaviour.**

## I. INTRODUCTION

Organic materials have been used to realize electro-active polymers (EAPs), because of their capabilities to transform electrical energy into mechanical energy and vice versa [1].

From studies on some organic materials, that present interesting propriety as conductors and semiconductors, a new technology has been developed in order to use organic materials in electronics circuit characterized by low cost manufacturing techniques and materials [2].

Moreover, EAPs have been proposed to obtain transducer that can work either as low-voltage motion actuators, if an electric field is applied across their thickness, or as motion sensors, generating a detectable voltage if subjected to a mechanical deformation. Starting from a transducers class belonging to EAP, Ionic Polymer Metal Composite (IPMC) [3], its structure has been modified in order to manufacture an all-organic transducers: Ionic Polymer-Polymer Composite (IP$^2$C) [4]. In details, their structure has been modified substituting the metal electrodes with organic conductor. A fluorocarbon membrane, Nafion®117, of thickness 178 µm (produced by Dupont and distributed by Sigma-Aldrich Group), is the core of IP$^2$Cs (Fig.1).


Fig. 1 Structure scheme of IP$^2$C.

The research activity presented in the paper has been supported by the PRIN project 'Innovative all-polymeric ionic transducers for post-silicon applications: realization, modeling, metrological characterization and applications' of the Italian Ministero dell'Istruzione dell'Università e della Ricerca.

The all-polymeric device presents electro-mechanical coupling capability with some interesting advantages than IPMC; in fact they require low cost manufacturing techniques and cheaper conductors than IPMC. Also, they are suitable to realize all-organic transduction systems, where both the electronic components and the transducers are realized by using organic components.

The device actuation is produced by applying an electric field between electrodes that generates a motion of free cations ($H^+$) through Nafion [5] membrane. Moreover, the solvent molecules are dragged by the free charges creating a displacement increment.

Although some publications are present in literature about the characterization as sensor [6] or as actuator of IP$^2$C, the full exploitation of IP$^2$C for the realization of motion actuators has not yet been possible because of some unsolved drawbacks. In these years, in fact many studies have been performed in order to improve deposition techniques of organic electrodes and device performances. Different problems have been tackled and solved, such as the organic electrodes layers adhesion and evaporation and electrolysis of generally used solvent (water) [7].

The considered IP$^2$C has been manufactured through a deposition technique of polymerization of PEDOT:PSS [8] that allows to obtain a good adhesion of electrodes. Moreover, ethylene glycol (EG) has been used in Nafion® membrane as solvent, in order to overcome the limitations due to water evaporation.

IP$^2$C modeling is needed to design suitable control system in a number of applications where the desired working conditions should be imposed. In [9] and in [10] two interesting applications of IPMC are developed where they are used to realize a resonant vibrating tactile probe and a tactile sensor respectively.

A set of experiments have been performed on the device in order to develop different models: a parametric grey-box model, a black-box ARX model and an Hammerstein-Wiener model (NLHW).

## II. EXPERIMENTAL SETUP AND DATA

Data used for model identification have been acquired during ad-hoc measurement surveys. The IP$^2$C membrane base has been put between two electrodes that allow to apply an input voltage, while the device tip is free to move. A

swept signal with amplitude 3 V and a frequency ranging from 20 mHz to 1 Hz has been applied, through a suitable conditioning circuit. The considered frequency values are representative of IP$^2$C working frequencies [11] with EG.

The input voltage applied to the membrane, along with its free deformation and absorbed current have been acquired through an acquisition card DAQ 6052 (National Instruments™) at a sampling frequency of 10 Hz. The displacement has been measured by means of a laser proximity sensor (Baumer Photoelectric sensor OADM 12). The experimental setup is shown in Fig. 2.

The data set (10000 data corresponding to1000s) obtained by applying the swept signal has been divided in an identification (Fig. 3(a)) and a validation data set. A sequence of step signals with different amplitude (Fig. 3(b)) has been also used to generate an independent validation data set. The persistence of excitation of the swept signal used to perform model identification has been verified.

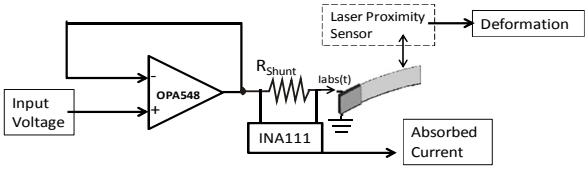


Fig. 2 The experimental setup for IP$^2$C electrical characterization: the OPA548 is a buffer used to apply the desired input voltage and to provide the absorbed current, which is measured by instrumentation amplifier INA111.

Though band limited noise white was used as an attempt to force the IP$^2$C based actuator, limits in the maximum allowed voltage input caused a very small deflection that was not suitable to perform the system identification.

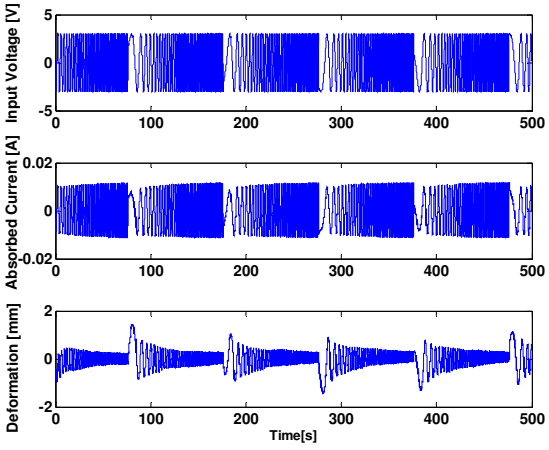


(a)

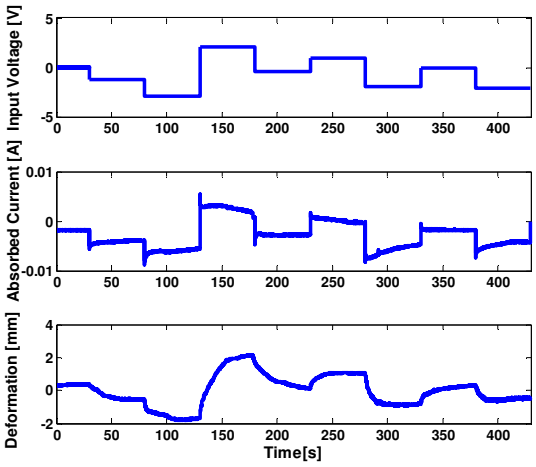


(b)

Fig. 3 The experimental data measured through the experimental setup: applied input voltage, absorbed current and deformation: (a) swept data and (b) step data.

## III. Gray and Black Box Models

Different models have been proposed in literature for IPMC [12][14][15]. Here, starting from some similarities that can be observed between IPMC and IP$^2$C behaviour, the model structure proposed for IPMC in [12] has been used as a starting point and has been adapted to IP$^2$C peculiarities.

### A. *Parametric model*

Starting from the considerations above, a linear model has been identified to simulate the IP$^2$C actuator behaviour. The model is composed by two blocks (Fig. 4) representing the electric and electromechanical subsystems.

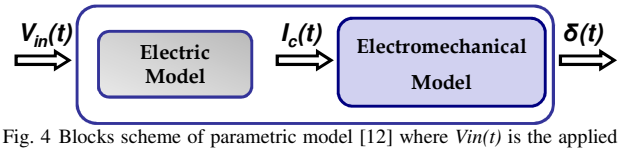


Fig. 4 Blocks scheme of parametric model [12] where *Vin(t)* is the applied input voltage, *Ic(t)* is the capacitive branches current (see Fig.5) and *δ(t)* is the corresponding free deformation.

The first step is to obtain the absorbed current from the applied voltage. An equivalent circuit was proposed to determine the electrical behavior of the device (Fig. 5). The current $i_{abs}(t)$ is evaluated summing the currents in the circuit branches: three capacitive ($R_2C_2$, $R_3C_3$ and $R_4C_4$) and a resistive one ($R_1$). The identification procedure, implemented in Matlab® environment, allows to determine resistance and capacitance values in order to minimize the error function (1), between experimental and simulated current. In Table I the identified values of circuit components are reported.

$$J_\delta = 100 \cdot \frac{\sqrt{\sum_i (ExperimentalData - ModelOutput)_i^2}}{\sqrt{\sum_i (ExperimentalData)_i^2}} \quad (1)$$

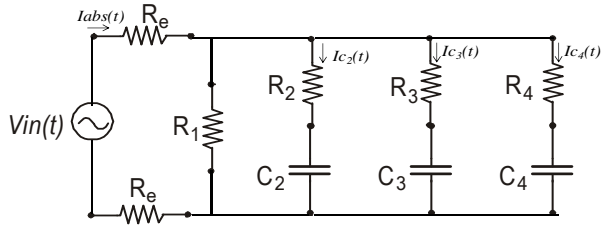


Fig. 5 Equivalent circuit of electric behaviour of IP$^2$C [14] where *Vin(t)* is the applied input Voltage, *Iabs(t)* is the measured absorbed current and $i_C(t) = i_{c2}(t)+i_{c3}(t)+ i_{c4}(t)$ is the input of electromechanical block.

TABLE I. IDENTIFIED VALUES.

| R2 | C2 | R3 | C3 | R4 | C4 | Re |
|---|---|---|---|---|---|---|
| 846Ω | 617μF | 1771Ω | 0.23mF | 501Ω | 0.38mF | 47Ω |

Still referring to Fig. 5, *R*1 is the equivalent bulk resistance of the Nafion® in DC conditions. It can be computed as a function of both the Nafion® DC resistivity $\rho 1$ and the geometrical dimensions of the samples, as reported in (2).

$$R1 = \frac{\rho_1 t}{L_t w} = 1.767\ k\Omega \quad (2)$$

where $L_t$ is the total length of the IP$^2$C and *w*, *t* are the dimensions of the IP$^2$C cross section (see Fig. 6 and Table II).

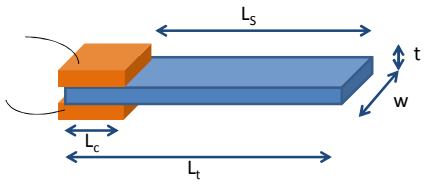


Fig. 6 IP$^2$C actuator device structure.

TABLE II. GEOMETRIC PARAMETERS OF IP$^2$C ACTUATOR

| $L_t$ | $L_s$ | $L_c$ | w | t |
|---|---|---|---|---|
| 30mm | 20mm | 10mm | 5mm | 220μm |

The absorbed current determines an IP$^2$C mechanical reaction due to the charges redistribution with the transport of some solvent molecules. More specifically, it is possible to evaluate the mechanical response of the membrane from the capacitive branches current, using a suitable electro-mechanical model.

The second stage of IP$^2$C model allows to estimate the deformation ($\delta(t)$) that the membrane produces because of the current $i_c(t)=i_{c2}(t)+i_{c3}(t)+ i_{c4}(t)$.

By considering the IPMC actuator model [14], the expression that links the membrane deformation with the capacitive current is reported in (3).

$$\frac{\delta(s)}{i_C(s)} = \frac{1}{s}\frac{3d(s)L_s^2}{\chi(s)L_t wt}\left(\frac{1}{1+s^2\frac{12L_s^4\rho}{\Gamma^4 Y(s)t^2}}\right) \quad (3)$$

where *Ls* is the total length without considering the length of the clamped part of the IP$^2$C. $\Gamma$ depends on the solution of the characteristic equation of the clamped beam for the first mode; its value is well known in the literature and is equal to 1.875 [13], $\rho$= 2100 kg/m$^3$ is the IP$^2$C density.

The term d(s) represents the coupling function between mechanical and electric domain and its estimation will be described in the following.

$\chi$(s) is the equivalent permittivity, it is the electrical impedance corresponding to the three capacitive branches of circuit of Fig. 5:

$$\chi(s) = \frac{\varepsilon_2}{1+s\varepsilon_2\rho_2} + \frac{\varepsilon_3}{1+s\varepsilon_3\rho_3} + \frac{\varepsilon_4}{1+s\varepsilon_4\rho_4} \quad (4)$$

$\varepsilon_2$, $\varepsilon_3$ and $\varepsilon_4$ are the dielectric constants of the capacitors $C_2$, $C_3$ and $C_4$, while $\rho_2$, $\rho_3$ and $\rho_4$ represent the resistivity in the branches. They can be evaluated by using of parameters values reported in Table I with the following expressions (with n=2,3,4):

$$\rho_n = R_n \frac{L_t w}{t} \quad (5)$$

$$\varepsilon_n = C_n \frac{t}{L_t w} \quad (6)$$

Y(s) represents the Young modulus and it has been estimated through the Dynamical Mechanical Analysis (DMA) of IP$^2$C samples by means of Tritec 2000 DMA.

Fig. 7 (a) and (b) show the experimental measurements of Storage and Loss Modulus that are required to evaluate the Young modulus (Y(s)= Storage Modulus + j Loss Modulus).

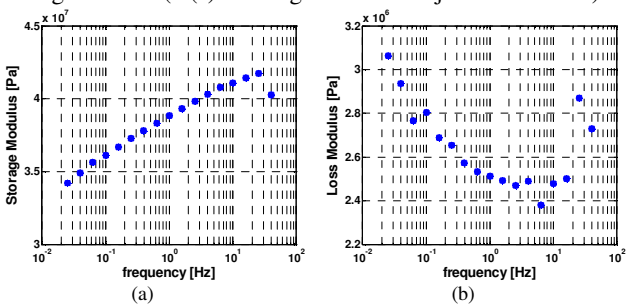


(a) (b)

Fig. 7 DMA measurements: (a) storage modulus and (b) loss modulus for IP$^2$C membrane.

A model of *Y(s)* has been derived by fitting the experimental data with a transfer function. After different

trials, the transfer function form that permitted a good fitting of the experimental data is reported in (7).

$$Y(s) = K_Y \frac{(s + z_{1Y})(s + z_{2Y})}{(s + p_{1Y})(s + P_{2Y})} \quad (7)$$

The parameters values in (7) have been obtained by minimization of the error function (1); they are reported in Table III.

TABLE III. PARAMETERS CHARACTERIZING THE YOUNG MODULUS.

| $K_y$ ($N \cdot m^{-2}$) | $p_{1y}(s^{-1})$ | $p_{2y}(s^{-1})$ | $z_{1Y}(s^{-1})$ | $z_{2Y}(s^{-1})$ |
|---|---|---|---|---|
| 4.11e+7 | 0.617 | 11.616 | 10.708 | 0.558 |

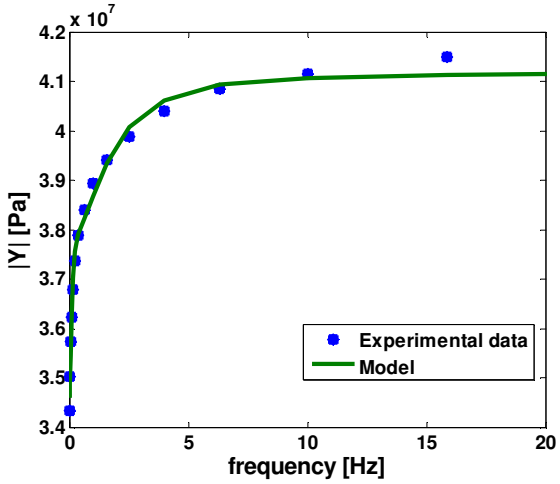


Fig. 8 Young modulus measurement and the corresponding model output.

Fig. 8 shows a comparison between the experimental data and the simulated modulus of (7).

The term d(s) represents the coupling function between mechanical and electric domain. The transfer function that allows to better fit experimental data is reported in (8).

$$d(s) = K_d \frac{1}{(s + p_{1d})(s + p_{2d})} \quad (8)$$

In Table IV the identified parameters of the coupling function obtained through the minimization of the function (1) are reported.

TABLE IV. PARAMETERS OF THE COUPLING FUNCTION.

| $k_d(C \cdot N^{-1} \cdot s^{-2})$ | $p_{1d}(s^{-1})$ | $p_{2d}(s^{-1})$ |
|---|---|---|
| 6.861e-006 | 0.6621 | 378.56 |

Considering (3), it is possible to rewrite the transfer function with respect to input voltage, evaluating the impedance Z* of the capacitive branches ($R_2$ $C_2$, $R_3$ $C_3$, $R_4$ $C_4$) and the resistive one (R1). The expression (9) is therefore obtained:

$$\frac{\delta(s)}{V_{in}(s)} = \frac{1}{s} \frac{3d(s)L_s^2}{\chi(s)L_t wt} \left( \frac{1}{1 + s^2 \frac{12L_s^4 \rho}{\Gamma^4 Y(s) t^2}} \right) \left( 1 - \frac{Z^*}{R_1} \right) \frac{1}{2R_e + Z^*} \quad (9)$$

In Fig. 9, Fig. 14 and Fig.15 the experimental data and corresponding model estimation are reported respectively for the first and second part of the swept signal and for the step sequences. The correlation coefficient between experimental data and simulated deformation, computed on the three data sets are reported in Table V.

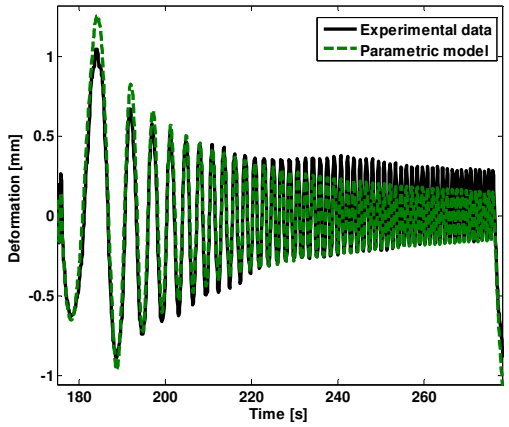


Fig. 9 Experimental *vs*. simulated free deformation computed on the estimation data.

### *B. ARX Model*

An ARX model of the system has been also identified from the experimental data.

Taking into consideration that the grey-box model has 9 poles and 5 zeros, we let the system order grow from 4 to 12. The Least Squares Algorithm [16] has been used to identify the model parameter in (10):

$$A(q)y(t) = B(q)u(t) + e(t) \quad (10)$$

Both the correlation between actual and simulated output, the residual analysis and the FPE criterion [16] have been used to select the best model. It is interesting to observe that best results have been obtained also in this case with the same pole-zero structure of the grey-box model.

The ARX one-step-ahead predictions computed on the two sets of validation data are reported in Fig.14 and Fig.15, while the corresponding predictions on the identification

data set is reported in Fig. 10. The corresponding correlation coefficients are listed in Table V.

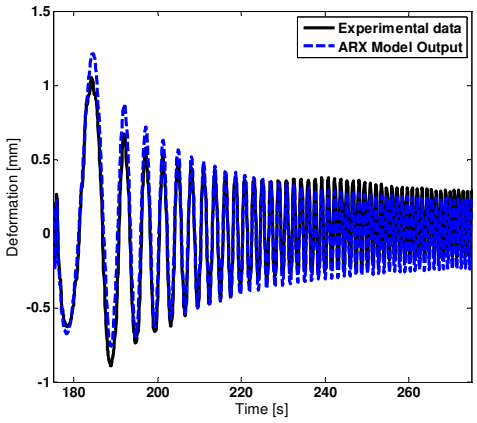


Fig. 10 Experimental vs. ARX one-step-ahead prediction of the free deformation computed on the identification data set.

### C. *Hammerstein-Wiener model*

To cope with possible static nonlinearities which have been found when modeling IPMC [12], a Hammerstein-Wiener model (NLHW) structure, reported in Fig. 11, has been identified.

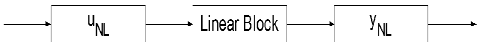


Fig. 11 Block diagram of Hammerstein-Wiener model: uNL and yNL are the static input and output nonlinerity.

Different nonlinearity shapes have been tried. Best results have been obtained with PWL nonlinearities. As shown in Fig. 12, the identified nonlinearities trends are not very significant. This is also reflected by the performance of NLHW model which gives only a modest improvement with respect to ARX model.

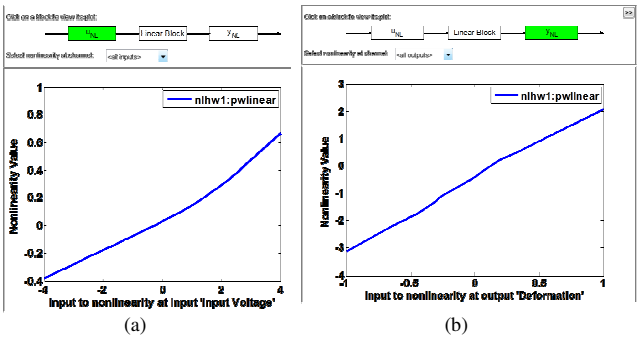


(a) (b)

Fig. 12 Nonlinearities in Hammerstein-Wiener model: (a) input and (b) output.

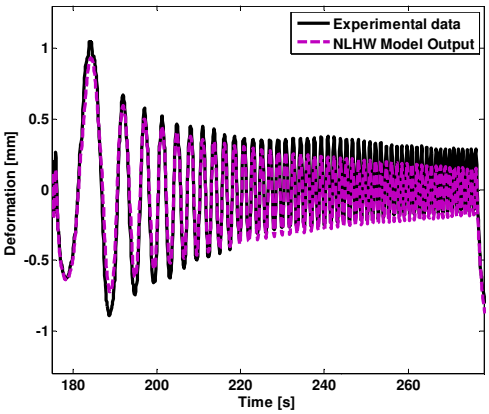


Fig. 13 Experimental vs. Hammerstein-Wiener model one-step-ahead prediction of the free deformation computed on the identification data set.

The one-step-ahead prediction of the Hammerstein-Wiener model is reported in Fig. 13, Fig. 14 and Fig. 15.

The corresponding correlation coefficients are reported in Table V.

## IV. Models Comparison

To compare the different models, in Table V and VI the correlation coefficients and the corresponding standard deviations between experimental deformations and the models output, computed both with the identification data and with the validation data, are reported.

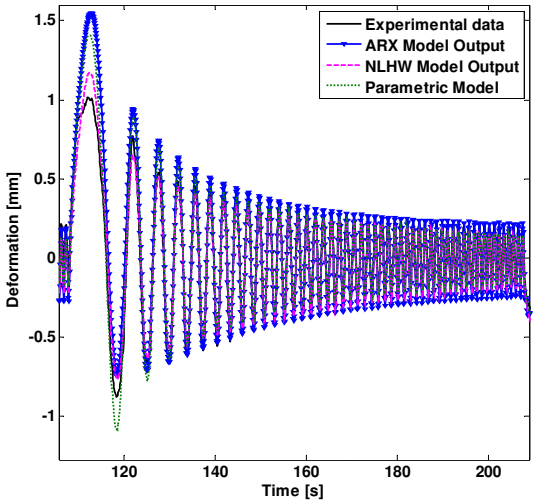


Fig. 14 Experimental vs. models simulated free deformation.

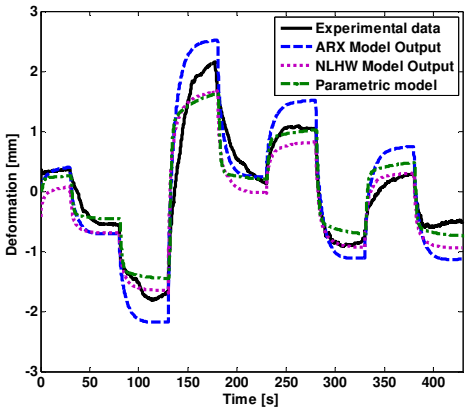


Fig. 15 Experimental vs. models simulated free deformation applying a sequence of step signals

TABLE V. CORRELATION COEFFICIENTS EVALUATED FOR COMPARING THE DEVELOPED MODELS WITH THE EXPERIMENTAL DATA

| | Grey Box Model | ARX Model | NLHW Model |
|---|---|---|---|
| Identification Swept Signal | 0.970 | 0.979 | 0.990 |
| Validation Swept Signal | 0.9574 | 0.9625 | 0.9733 |
| Validation Step signal | 0.9448 | 0.970 | 0.957 |

TABLE VI. STANDARD DEVIATIONS EVALUATED FOR COMPARING THE DEVELOPED MODELS WITH VALIDATION EXPERIMENTAL DATA.

| | Grey Box Model | ARX Model | NLHW Model |
|---|---|---|---|
| Identification Swept Signal | 0.099 | 0.0847 | 0.0805 |
| Validation Swept Signal | 0.1137 | 0.1162 | 0.0873 |
| Validation Step signal | 0.3158 | 0.418 | 0.275 |

## V. CONCLUSION

In this paper different models of IP$^2$C used as actuators have been investigated. Both a gray-box modeling approach and black-box models identification have been applied to the same sets of experimental data. The results obtained show that an improvement is obtained by using black box strategies. Moreover, the introduction of the static nonlinearity in the ARX model produced a small improvement.

Though black-box models worked slightly better than the grey- box model, they do not allow to have a clear physical meaning of the identified parameters. The black-box approach selected a model with the same pole-zero structure of the grey-box model. This gives evidences of the correctness of the general structure conjectured for the gray-box model. Further investigation can be performed both to improve the grey-box model and to identify NARX models.

## ACKNOWLEDGMENT

The authors acknowledge Prof. G. Di Pasquale that produced IP$^2$C samples.

## REFERENCES

[1] Yoseph Bar-Cohen, "Electro-active polymers: current capabilities and challenges", Proceedings of the SPIE Smart Structures and Materials Symposium, EAPAD Conference, San Diego, CA, March 18-21, 2002.

[2] K. Iniewski, "Nanoelectronics: Nanowires, Molecular Electronics, and Nanodevices" Mc Graw Hill, 2010.

[3] M. Shahinpoor and J. K. S. Kim, "Ionic polymer–metal composites: I. Fundamentals", Smart Mater. Struct.,vol. 10, 819–833, 2001

[4] L. Fortuna, S. Graziani, M. La Rosa, D. Nicolosi, G. Sicurella, E. Umana, "Modeling and design of all-organic electromechanic transducers", IS-FOE'08 special issue, European Physical Journal – Applied Physics (EPJ-AP), vol.46, no.1, pp.12513 (p1-p4), 2009.

[5] www.doitpoms.ac.uk/tlplib/fuel-cells/pem_membrane.php

[6] G. Di Pasquale, L. Fortuna, S. Graziani, M. La Rosa, D. Nicolosi, G. Sicurella, E. Umana, "All-organic motion sensors: characterization and modeling", IEEE Transaction on Instrumentation and Measurement (I2MTC'08 Special Issue), vol. 58, Issue 10, pp. 731 – 3738, 2009.

[7] G. Di Pasquale, L. Fortuna, S. Graziani, M. La Rosa, A. Pollicino and E. Umana,"A study on IP2C actuators using ethylene glycol or EmI-Tf as solvent" IOP -Smart Materials and Structures, vol. 20 , 045014 (9pp), 2011.

[8] S. J. Higgins, K. V. Lovell, R. M. G. Rajapakse and N. M. Walsby" Grafting and electrochemical characterisation of poly-(3,4-ethylenedioxythiophene) films, on Nafion and on radiation-grafted polystyrenesulfonate–polyvinylidene fluoride composite surfaces", J. Mater. Chem., 13, 2485 – 2489, 2003.

[9] P. Brunetto, L. Fortuna, P. Giannone, S. Graziani, F. Pagano, "A resonant vibrating tactile probe for biomedical applications based on IPMC", IEEE Transaction on Instrumentation and Measurement, vol.59 Issue 5,pp. 1453 - 1462

[10] C. Bonomo, P. Brunetto, L. Fortuna, P. Giannone, S. Graziani and S. Strazzeri "A Tactile Sensor for Biomedical Applications Based on IPMCs, IEEE Sensors Journal, vol.8, no.8, 2008, pp.1486-1493

[11] Surya Darma Pandita, Hyoung Tae Lim, Young Tai Yoo, Hoon Cheol Park, "The Actuation Performance of Ionic Polymer Metal Composites with Mixtures of Ethylene Glycol and Hydrophobic Ionic Liquids as an Inner Solvent", *Journal of the Korean Physical Society*, Vol. 49, No. 3, September 2006, pp. 1046-1051.

[12] C. Bonomo, L. Fortuna, P. Giannone, S. Graziani, S. Strazzeri: A nonlinear model for ionic polymer metal composites as actuators, Smart Mater. and Struct, 16, 1-12(12), 2007.

[13] Scott Whitney "Vibration of Cantilever Beams: Deflection, Frequency and Research Uses, EngrM 325H, 1999.

[14] P. Brunetto, L. Fortuna, P. Giannone, S. Graziani, S. Strazzeri, "Optimization of IPMC Actuators Conversion Efficiency", Advances in Science and Technology Vol. 6,1 pp 131-140, 2008.

[15] K. M. Newbury and D. J. Leo: Elecromechanical modeling and chaeracterization of ionic polymer benders, J. Intell. Mater. Syst. Struct. 13 51–60, 2002;

[16] Lennart Ljung,"System Identification-Theory For the User" 2nd ed, PRT Prentice Hall, Upper Saddle River, N.J., 1999.